



Article

# Novel Liquid Biomarker Panels for A Very Early Response Capturing of NSCLC Therapies in Advanced Stages

Florian Janke <sup>1,2,3,4,†</sup>, Farastuk Bozorgmehr <sup>3,5,†</sup>, Sabine Wrenger <sup>6,7</sup>, Steffen Dietz <sup>1,3</sup>,  
Claus P. Heussel <sup>3,8,9</sup>, Gudula Heussel <sup>3,8,10</sup>, Carlos F. Silva <sup>3,8,9</sup>, Stephan Rheinheimer <sup>3,8,9</sup>,  
Manuel Feisst <sup>11</sup>, Michael Thomas <sup>3,5</sup>, Heiko Golpon <sup>7,12</sup>, Andreas Günther <sup>13,14</sup>,  
Holger Sültmann <sup>1,2,3</sup> , Thomas Muley <sup>3,15</sup>, Sabina Janciauskiene <sup>6,7</sup>, Michael Meister <sup>3,15</sup> and  
Marc A. Schneider <sup>3,15,\*</sup> 

<sup>1</sup> Division Cancer Genome Research, German Cancer Research Center (DKFZ), INF 280, 69120 Heidelberg, Germany

<sup>2</sup> German Cancer Consortium (DKTK), INF 280, 69120 Heidelberg, Germany

<sup>3</sup> Translational Lung Research Center Heidelberg (TLRC), Member of the German Center for Lung Research (DZL), INF 156, 69120 Heidelberg, Germany

<sup>4</sup> Medical Faculty, Heidelberg University, 69117 Heidelberg, Germany

<sup>5</sup> Department of Thoracic Oncology, Thoraxklinik at University Hospital Heidelberg, Roentgenstrasse 1, 69126 Heidelberg, Germany

<sup>6</sup> Department of Respiratory Medicine, Hannover Medical School, Carl-Neuberg-Str. 1, 30625 Hannover, Germany

<sup>7</sup> Biomedical Research in Endstage and Obstructive Lung Disease Hannover (BREATH), Member of the German Center for Lung Research (DZL), Carl-Neuberg-Str. 1, 30625 Hannover, Germany

<sup>8</sup> Department of Diagnostic and Interventional Radiology with Nuclear Medicine, Thoraxklinik at University Hospital Heidelberg, Roentgenstrasse 1, 69126 Heidelberg, Germany

<sup>9</sup> Department of Diagnostic and Interventional Radiology, University Hospital Heidelberg, INF 400, 69120 Heidelberg, Germany

<sup>10</sup> Department of Pneumology, Thoraxklinik at University Hospital Heidelberg, Roentgenstrasse 1, 69126 Heidelberg, Germany

<sup>11</sup> Institute of Medical Biometry and Informatics (IMBI), University of Heidelberg, Im Neuenheimer Feld 130.3, 69120 Heidelberg, Germany

<sup>12</sup> Department of Pneumology, Hannover Medical School, Carl-Neuberg-Str. 1, 30625 Hannover, Germany

<sup>13</sup> Cardio-Pulmonary Institute (CPI), Klinikstr. 33, 35392 Giessen, Germany

<sup>14</sup> Universities of Giessen and Marburg Lung Center (UGMLC), Member of the German Center for Lung Research (DZL), Klinikstr. 33, 35392 Giessen, Germany

<sup>15</sup> Translational Research Unit, Thoraxklinik at University Hospital Heidelberg, Roentgenstrasse 1, 69126 Heidelberg, Germany

\* Correspondence: marc.schneider@med.uni-heidelberg.de; Tel.: +49-6221-3961665; Fax: +49-6221-3961652

† These authors contributed equally to this work.

Received: 16 March 2020; Accepted: 10 April 2020; Published: 12 April 2020



**Abstract:** Computed tomography (CT) scans are the gold standard to measure treatment success of non-small cell lung cancer (NSCLC) therapies. Here, we investigated the very early tumor response of patients receiving chemotherapy or targeted therapies using a panel of already established and explorative liquid biomarkers. Blood samples from 50 patients were taken at baseline and at three early time points after therapy initiation. DNA mutations, a panel of 17 microRNAs, glycodelin, glutathione disulfide, glutathione, soluble caspase-cleaved cytokeratin 18 (M30 antigen), and soluble cytokeratin 18 (M65 antigen) were measured in serum and plasma samples. Baseline and first follow-up CT scans were evaluated and correlated with biomarker data. The detection rate of the individual biomarkers was between 56% and 100%. While only keratin 18 correlated with the tumor load at baseline, we found several individual markers correlating with the tumor response to treatment

for each of the three time points of blood draws. A combination of the five best markers at each time point resulted in highly significant marker panels indicating therapeutic response ( $R^2 = 0.78$ ,  $R^2 = 0.71$ , and  $R^2 = 0.71$ ). Our study demonstrates that an early measurement of biomarkers immediately after therapy start can assess tumor response to treatment and might support an adaptation of treatment to improve patients' outcome.

**Keywords:** NSCLC; early response biomarkers; liquid biomarkers; targeted therapy; chemotherapy

---

## 1. Introduction

Lung cancer is the most common cause of cancer-related death worldwide with non-small cell lung cancer (NSCLC) being the predominant entity with approximately 85% of cases [1]. Treatment options have changed considerably within the past years, especially with the advent of tyrosine-kinase-inhibitors (TKI) for epidermal growth factor receptor (EGFR) mutation and anaplastic lymphoma kinase (ALK) rearrangement positive NSCLC, which comprises about 15% and 2% of NSCLC cases, respectively [2,3]. TKI therapies result in substantial survival benefits for the patient [4–6]. However, most patients eventually experience relapse as a result of acquired TKI resistance [7,8]. For patients without targetable mutations, platinum-based chemotherapy ( $\pm$ pembrolizumab) is still the treatment of choice, except for patients with programmed death ligand 1 (PDL1) expression  $>50\%$ , who can receive immunotherapy with pembrolizumab as a monotherapy.

Regardless of the type of therapy, the gold standard for clinical monitoring of therapy efficacy in lung cancer patients is change in tumor size according to Response Evaluation Criteria in Solid Tumors, version 1.1 (RECIST-1.1) criteria. However, these changes are often evident in CT and MRI imaging with a delay of several weeks after initiation of systemic treatment and, therefore, unsuitable for frequent therapy monitoring and early assessment of response. The analysis of circulating biomarkers such as circulating tumor DNA (ctDNA), circulating microRNAs (miRNAs), and disease-associated protein markers offers a minimal-invasive tool to overcome this limitation, permitting frequent sample collection and timely assessment of the patient's disease status. This would allow for early detection of non-responders and avoid side effects and costs of ineffective treatment.

Preclinical and clinical studies have shown that apoptosis significantly increases 24 h after chemotherapy administration [9–11]. These changes in tumor biology are expected to result in changes in plasma/serum levels of (i) defined proteins relating to tumor cell death and regressions and (ii) release of free DNA, RNA carrying mutations and/or gene fusions.

Previous studies have shown that *EGFR* mutations can be detected in the plasma of patients with high prevalence, reflecting the landscape and heterogeneity of primary tumors and metastases in NSCLC [12,13]. Serial evaluation of mutant DNA could provide a noninvasive assessment of therapy response and tumor progression, including the detection of resistance mutations or an increase of *EGFR* sensitizing mutations associated with clinical progression.

MicroRNAs are short noncoding RNA molecules known as important regulators of gene expression. Deregulation of miRNAs is frequently observed in human cancers, including lung cancer, and is considered one of the characteristics of malignant transformation [14]. With their high stability, circulating miRNAs can be detected robustly in plasma and, therefore, represent promising biomarkers in cancer patients [15,16].

Another sign of tumor cells undergoing apoptosis is the increase of caspase-cleaved cytokeratin 18 fragments (M30 antigen). In the circulation, CK-18 occurs as a full-length protein (M65 antigen) as well as the 21-kDa caspase-cleaved fragment if epithelial cells undergo apoptosis [17]. Previous studies have demonstrated that serum levels of CK-18 proteins can be useful as an independent factor in predicting response to chemotherapy in patients with NSCLC [18].

Glutathione (GSH) is a tripeptide of glutamate, cysteine, and glycine, a potent antioxidant found at high concentration in all tissues. Under normal conditions, the majority of GSH exists in reduced form (0.5 to 10 mM). However, when GSH interacts with free radicals or acts as a cofactor for antioxidant enzymes, such as GSH peroxidases, oxidized glutathione (oxGSH) is generated [19]. Increased glutathione levels and glutathione-S-transferase activity have been implicated in platinum neutralization and resistance. The correlation between increased glutathione levels and drug resistance has been documented in a variety of tumors [20].

A further target used in this study was the glycoprotein glycodeilin, which has been well characterized in females [21]. It is secreted by the inner layers of the endometrium and highly expressed during the first trimester of pregnancy. Glycodeilin has been shown to regulate the invasion of the trophoblast into the endometrium and the immunotolerance of the maternal immune system [22]. However, several studies have demonstrated the expression and of glycodeilin in hormone-regulated cancers, i.e., ovarian cancer [23] and breast cancer [24], as well as in non-hormone-regulated cancers such as melanoma [25] and lung cancer [26].

This study aimed to define predictive marker panels indicating a successful or failing tumor therapy at very early time points after therapy initiation. Therefore, each of the described biomarkers was evaluated separately and in combination for their potential as predictive therapy markers at very early time points (day +1, day +7, day +14) in patients with advanced NSCLC.

## 2. Results

### 2.1. Biomarker Detection

For this study, we collected serum and plasma from 50 NSCLC patients. Patients were divided into two groups depending on disease treatment. Group A ( $n = 25$ ) received conventional chemotherapy since no targetable molecular alteration was detected during routine diagnostics. Group B ( $n = 25$ ) consisted of patients with a driver mutation or gene fusion targetable with a tyrosine kinase inhibitor (see patients' characteristics, Table 1). First blood sample was collected within 24 h prior to therapy start (day  $-1$ , Figure 1). Due to different therapy concepts, blood samples were collected at different time points after therapy start. For the chemotherapy group (group A), one post-treatment sample was collected at day +1, while two blood samples were assembled at day +7 and +14 for the TKI group (group B). In the first approach, patients' tumor response to therapy was assessed (Figure 2A). The TKI patients (group B) showed better therapy response compared to patients treated with chemotherapy. Using RECIST-1.1 criteria, 21 of the 50 patients revealed a response to therapy with a partial remission. For two patients, progress of the disease was diagnosed at the time of follow-up.

**Table 1.** Patient characteristics.

Parameter	n	(%)
median age in years (range)	62 (40–84)	
gender	50	100
male	24	48
female	26	52
ECOG	50	100
0	25	50
1	21	42
no data	4	8
Smoking status	50	100
current smoker	17	34
ex-smoker <6 months	4	8
ex-smoker >6 months	17	34
non-smoker	10	20
no data	2	4
histology	50	100
non-small cell lung cancer	50	100
adenocarcinoma	46	92
squamous cell carcinoma	1	2
large cell carcinoma	1	2
NOS	2	4
clinical stage (8th edition)	50	100
stage IVA	21	42
stage IVB	29	58
therapy	50	100
chemotherapy *	25	50
targeted therapy	25	50
EGFR **	20	40
EML4-ALK ***	4	8
BRAF	1	2

ECOG: Eastern Cooperative Oncology Group Performance Status Scale, NOS: non other specified, EGFR: Epidermal Growth Factor Receptor, EML4-ALK: echinoderm microtubule associated protein-like 4-anaplastic lymphoma kinase: BRAF: Serine/threonine-protein kinase B-raf (rapidly accelerated fibrosarcoma). \* 20 patients received Carboplatin/Pemetrexed, 3 patients Cisplatin/Pemetrexed, 1 patient Carboplatin/nab-Paclitaxel, 1 patient received Cisplatin/Alimta/Avastin. \*\* 12 patients received afatinib, 6 patients erlotinib, 1 patient gefitinib, 1 patient received nazartinib/capmatinib. \*\*\* 2 patients received alectinib, 2 patients received crizotinib. The BRAF patient received trametinib.

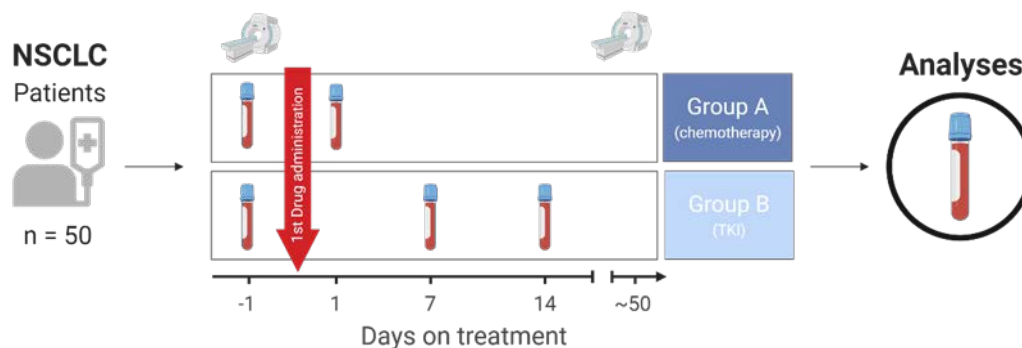


**Figure 1.** Description of the study concept. Blood from 50 patients with non-small cell lung cancer (NSCLC) was collected at baseline one day prior to therapy start (day −1) and after therapy initiation (day +1 for group A, day +7 and +14 for group B). Routine computer tomography (CT) at baseline and at time point of first clinical restaging was evaluated for tumor load change. Restaging CT was assessed in median at day 50. TKI: tyrosine kinase inhibitor.

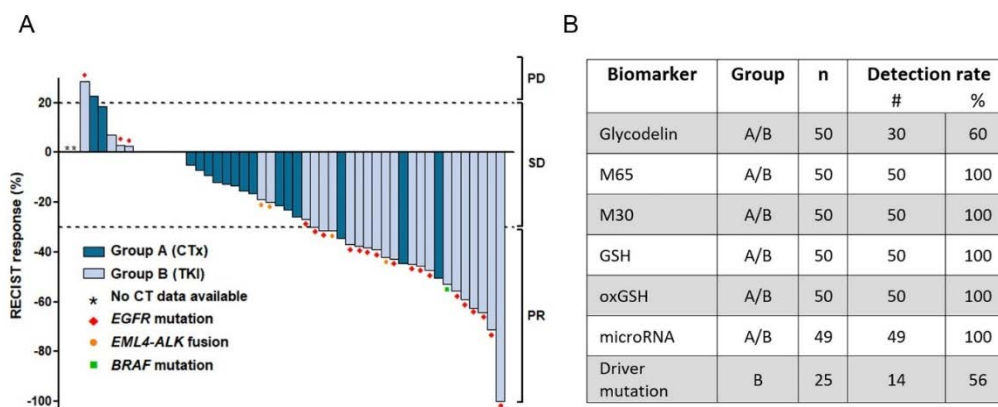


**Figure 2.** Patient response and detection rates of biomarkers. **(A)** Waterfall plot of tumor response to therapy. Tumor load was evaluated by an experienced radiologist using Response Evaluation Criteria in Solid Tumors, version 1.1 (RECIST-1.1) criteria. Dotted lines indicate thresholds for definition of progressive disease (PD), stable disease (SD), or partial remission (PR). Group A included patients treated with platinum-based chemotherapy, group B consists of patients receiving targeted therapy. **(B)** Detection efficiency of the biomarkers measured in both groups. CTx: Platinum-based chemotherapy, TKI: Tyrosine kinase inhibitor, EGFR: Epidermal Growth Factor Receptor, EML4-ALK: echinoderm microtubule associated protein-like 4-anaplastic lymphoma kinase, BRAF: Serine/threonine-protein kinase B-raf (rapidly accelerated fibrosarcoma), M65: Intact and caspase-cleaved Cytokeratin 18, M30: caspase-cleaved Cytokeratin 18, GSH: Glutathione, oxGSH: Oxidized glutathione.

Fifteen patients had a slightly lower tumor load, six patients exhibited a stable tumor load, and four patients exhibited a slight progression of the tumor diagnosed as stable disease. The investigated biomarkers (Table 2 and Appendix A Table A1) were detected in 100% of the patient groups, except glycodelin (60%) and the driver mutation of the TKI group (56%) (Figure 2B). Quality control for mutation detection and RNA measurements revealed that the investigated plasma samples had no or only a low risk to be affected by hemolysis (Table A2). For two patients from group A, no CT data were available, and for another patient from group B, miRNA analyses and mutation detection failed due to low amount of blood sample. These three patients were excluded from the subsequent analyses.

**Table 2. Biomarkers.** Overview of investigated biomarkers.

Biomarker	Application in Liquid Biopsy	References	Group
Glycodelin	Glycodelin is secreted by non-small cell lung cancer (NSCLC) cells and has predictive value when measured in the serum of patients.	[26,27]	A/B
Cytokeratin-18	Full length (M65) and caspase-cleaved (M30) forms of cytoke- ratin-18 are increased in lung cancer patients and correlate with apoptosis.	[17,28,29]	A/B
	Glutathione (GSH) and oxidized glutathione (oxGSH) protect cancer cells against cytotoxic compounds and are overexpressed in NSCLC cell lines.	[30,31]	A/B
microRNA	Deregulation of miRNA is associated with various diseases including cancer. Circulating miRNAs show variable abundances in lung cancer patients and healthy individuals, which may be useful for diagnosis, prognosis, and therapy monitoring. An overview of the miRNAs selected for this study is provided in Table A1.	[32,33]	A/B
Driver mutation	Mutations detectable in circulating DNA can reflect the landscape of primary tumors and metastases. Serial evaluation of mutant DNA could provide a noninvasive assessment of therapy response.	[34,35]	B

## 2.2. Correlation of Tumor Load and Biomarker Detection at Time Point of Therapy Start

First, we were interested in whether the serum/plasma levels of the selected biomarkers correlate with tumor load at the time of diagnosis (Figure 3A). The tumor load was assessed by an experienced radiologist and defined as the size of the tumor(s) at the time point of therapy start. Afterward, the different biomarkers were determined and correlated to tumor load using Pearson correlation coefficient. Interestingly, the plasma levels of biomarkers M30 and M65 (cleaved and full-length cytokeratin 18) correlated significantly with the tumor load of the patients ( $r = 0.55$ ,  $p < 0.001$  and  $r = 0.42$ ,  $p = 0.002$ , Figure 3B). All other markers failed to correlate in our cohort at the time of diagnosis.

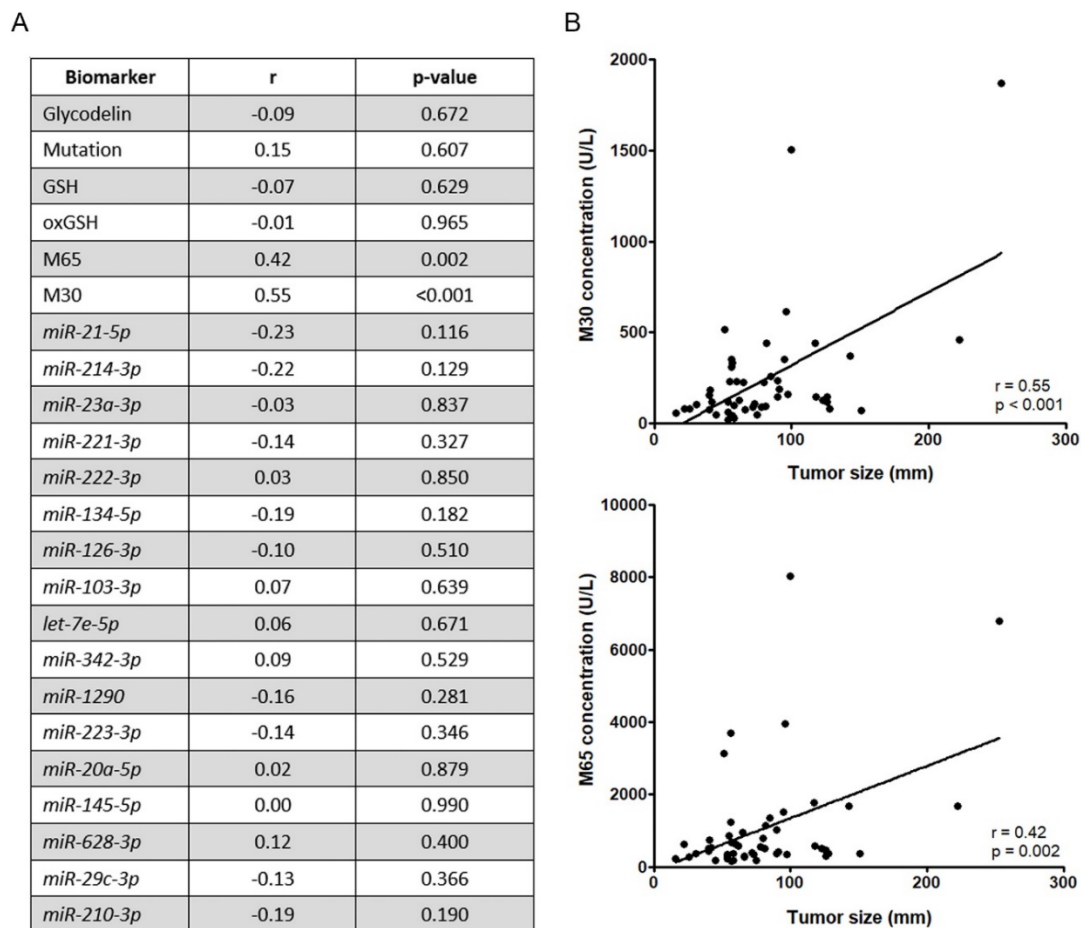


**Figure 3.** Correlation of markers and tumor load at baseline. (A) Linear regression analyses of the individual biomarkers and the tumor load at baseline time point. (B) Correlation plots of the two biomarkers with the highest correlation (M30 and M65).

## 2.3. Correlation Analyses of Single Biomarkers and Tumor Load Change

To investigate whether each of the biomarkers can individually indicate an early response to therapy, we first correlated every single marker with the change of tumor load. To do so, we examined the predictive value of the single markers in serum and plasma at the three time points using a linear regression model comprising the variable “relative tumor load change from baseline to first CT after therapy” (Figure 4). For group A, the microRNA *hsa-miR-210-3p* significantly correlated with the tumor load change ( $r = 0.49$ ,  $p = 0.017$ ), while for group B (day +7) *hsa-miR-134-5p* showed the best correlation with the tumor load change ( $r = -0.47$ ,  $p = 0.020$ ). *hsa-miR-23a-3p* and *hsa-miR-134-5p* also correlated partly ( $r = -0.43$ ,  $p = 0.036$  and  $r = -0.41$ ,  $p = 0.049$ ). For group B, the mutation detected in cell-free DNA (cfDNA) correlated best ( $r = 0.61$ ,  $p = 0.020$ , Figure 4). Using Pearson correlation coefficient,

heatmaps combining every single marker also revealed that there are highly correlated biomarkers at every time point, for example, M65 and M30.

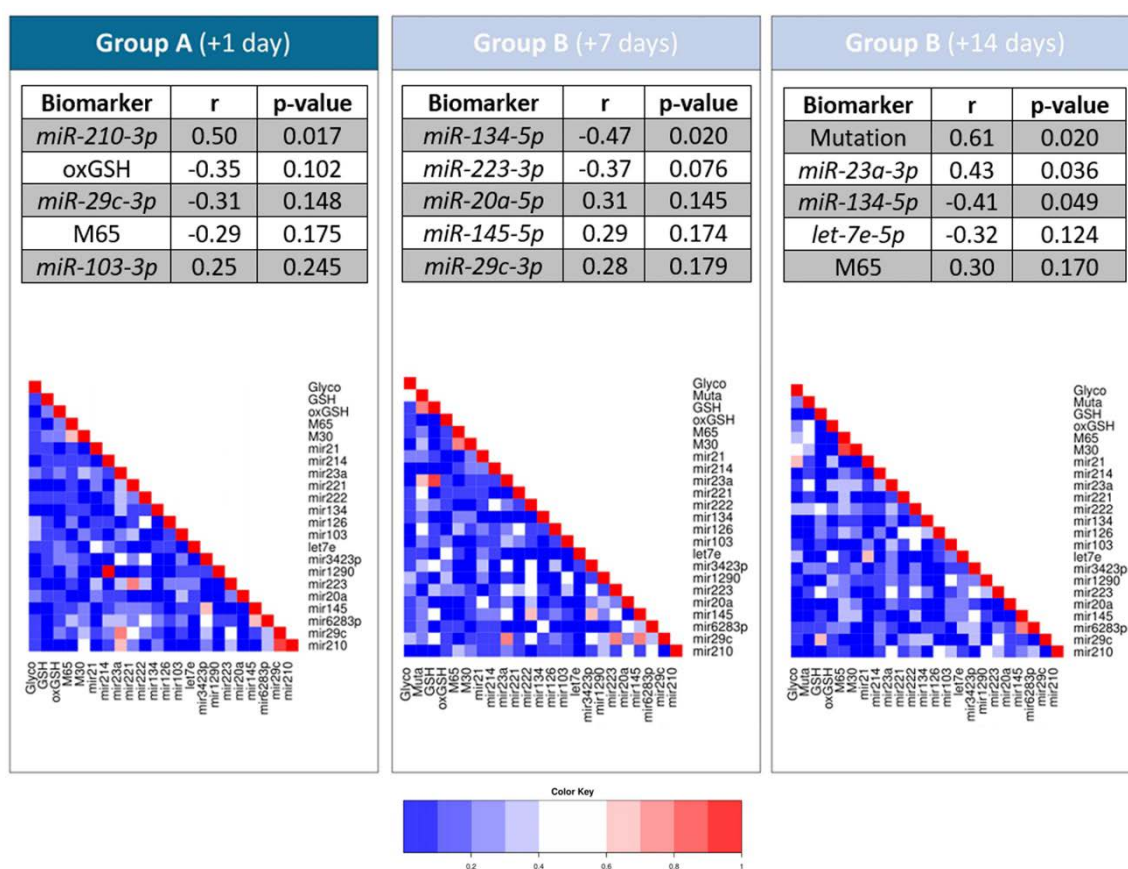


**Figure 4.** Predictive value of single markers at the three time points and correlation analyses. Linear regression analysis results of the individual markers at the three time points in relation to relative tumor load change from baseline to first CT after therapy. Heatmap indicates correlation between the single biomarkers (Pearson correlation).

#### 2.4. Stepwise Regression Model

Many different markers have been described to be useful individually for diagnosis or prediction of NSCLC therapies [36]. However, due to complex biological changes in tumor and patients' metabolism, no single biomarker has entered clinical routine. Hypothesizing that a marker panel might be superior to single markers, we performed a five-step forward regression analysis (based on the Akaike Information Criterion) to find a marker panel consisting of the 23 investigated biomarkers with the best predictive performance for each time point (Figure 5). Using marker panels, the correlation of the tumor load change and the marker abundance change increased to  $R^2 = 0.78$  (group A, time point +1),  $R^2 = 0.71$  (group B, time point +7), and  $R^2 = 0.71$  (group B, time point +14) (Figure 5A). Thereby, *hsa-miR-20a-5p* was the only marker included in more than one panel. Interestingly, none of the individual biomarker panels was predictive at the other investigated time points (Table A3). As an example, while the marker panel for group B at day +7 correlated well with the tumor load change ( $R^2 = 0.71$ ), a low correlation was observed for group A at day +1 ( $R^2 = 0.06$ ) and for group B at day +14 ( $R^2 = 0.25$ ). Visualization of each panel showing the marker abundance change in relation to tumor load change confirmed the strengths of the individual panels (Figure 5 B).

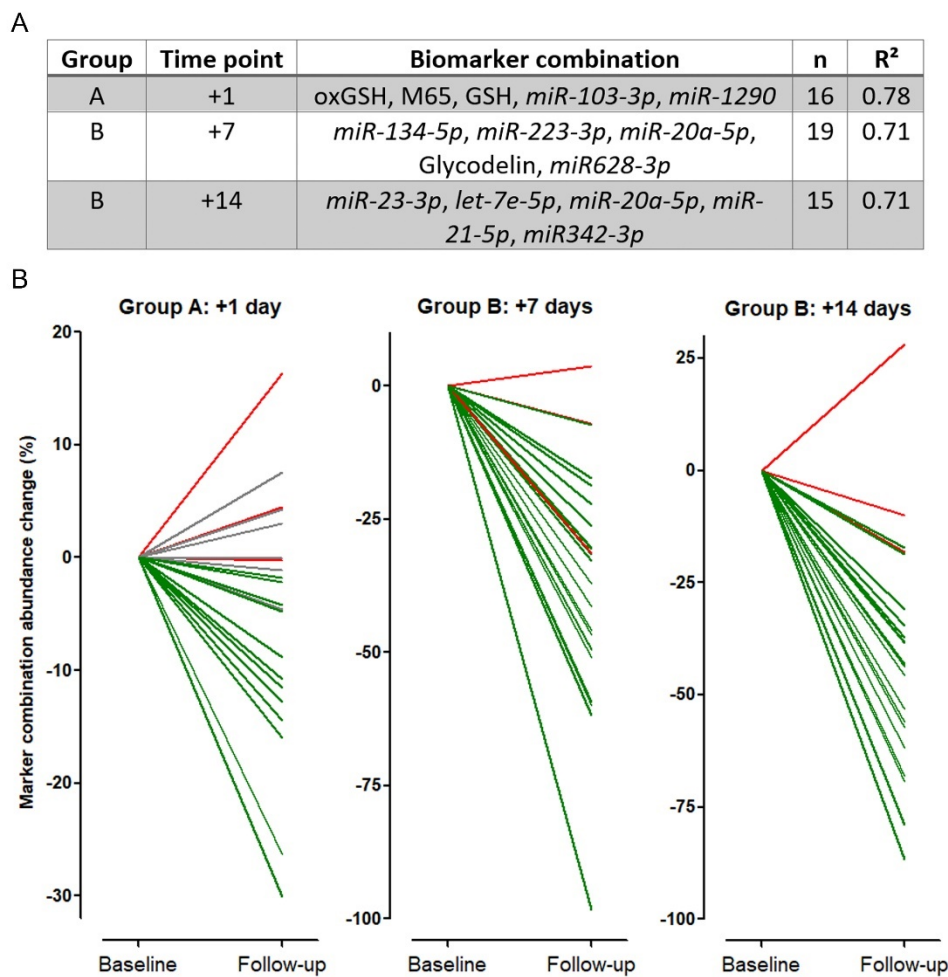


**Figure 5.** Stepwise regression model and marker combination abundance change. (A) Five-step forward regression analysis using the five best markers for each time point. (B) Biomarker combination from (A) in relation to tumor load change. Every line represents one patient. green = patients with tumor load reduction, red = patients with tumor growth, grey = patients without tumor load change at first CT scan after therapy start.

Tumor load change for each patient from baseline to follow-up was indicated in green (reduced tumor load), grey (no tumor load change), and red (increased tumor load change). While all patients with a lower marker panel value also had a reduced tumor load (green lines), only patients with no (grey lines) or increased (red lines) tumor load change showed an increased marker panel abundance change. Using the three best markers instead of the five markers panel resulted in a decrease of predictive robustness ( $R^2 = 0.62$  for group A, time point +1;  $R^2 = 0.61$  for group B, time point +7, and  $R^2 = 0.54$  for group B, time point +14).

### 3. Discussion

The field of biomarkers in NSCLC is very diverse with a variety of methods and biomarkers investigated in the past. Besides classical tissue-based markers that have been used for decades [37], modern methods analyzing proteomes, epigenomes, or metabolomes enlarged the generally available biomarker resources [38]. Liquid biopsies have attracted increasing attention in recent years for disease diagnosis, prognosis, and treatment, especially in late stages and with poor general condition of the patients [39]. An early assessment of liquid biomarkers has demonstrated that changes in circulating tumor DNA (ctDNA) or microRNA levels might indicate therapy response [40–42].



The current study was conducted to investigate whether a very early assessment of different blood-based biomarkers might indicate a tumor response to therapy. We selected 23 biomarkers that have been shown to be relevant in liquid biopsy approaches, including prognosis or therapy response. These markers were measured in two patient groups (group A,  $n = 25$ , chemotherapy cohort and group B,  $n = 25$ , TKI cohort). Considerable hemolysis, which might influence the quality and composition of the investigated microRNAs [43], was not observed in the plasma samples of our cohort. Glycodelin, which has been described as a prognostic liquid biomarker in NSCLC, was detectable in only 60% of all samples. This is in line with literature data where it was demonstrated that glycodelin is measurable only in particular serum samples [27]. Similar observations were made for ctDNA. Here, the detection rate in group B was only 56%. This might be explained by the fact that the ctDNA is markedly diluted by circulating germline DNA. Similar rates have been published investigating EGFR resistance mutations in liquid biopsies [35,44,45]. Interestingly, nearly all investigated markers failed to correlate with the tumor load at baseline. Contrary to our expectations, although the copy number of mutations and the glycodelin serum concentrations correlated within group B at time point +7, the biomarkers glycodelin and the driver mutation abundance did not correlate with the tumor size. We expected a correlation since both markers are exclusively expressed and released by malignant cells. Only the apoptosis markers M65 and M30 (full-length and cleaved cytokeratin 18) correlated with tumor load and might be useful markers for diagnosis, which confirms published data [46].

The analysis of biomarker abundance and change of tumor load revealed that for group A (day +1) and group B (day +7) only one microRNA each (*miR-210-3p* and *miR-134-5p*) was significant. This is in line with published data since *miR-210-3p* has been described to be a marker decreasing after chemotherapy treatment of patients with NSCLC, while *miR-134-5p* is upregulated in gefitinib resistance cell lines. For day +14 (group B), three out of the 23 biomarkers correlated significantly with the tumor load change. Here, the mutational status was the best marker at this time point. In addition, *miR-23a-3p* and *miR-134-5p* were also found to be significant predictors for tumor response to treatment at day +14 after therapy initiation. Since our cohort size was limited and our goal was to define a marker panel for valid evidence, we performed a stepwise forward regression model with the five most promising biomarkers for each time point. Indeed, we reached a very high model fit for all three measured groups ( $R^2 = 0.78$  (day +1),  $R^2 = 0.71$  (day +7 and +14)) considering the relatively small cohort size. Due to this statistical method and the fact that glycodelin as well as the driver mutation were not detectable in all patients, the number of patients included in the analyses dropped down from 25 to  $n = 16$  (day +1),  $n = 19$  (day +7), and  $n = 15$  (day +14) in the three groups. Using a panel consisting of five markers in this relatively small cohort, therefore, might indicate an overfitted model. However, a reduction to a three-marker based panel still reached high predictive values at the three time points ( $R^2 = 0.62$  (day +1),  $R^2 = 0.61$  (day +7), and  $R^2 = 0.54$  (day +14)). We also observed that the marker panels cannot be transferred to the other time points of blood sample collection. On the one hand, this might result from different cellular processes since the time between the three blood assessments was approximately one week each. The complex interaction of cellular therapy response, as well as apoptotic processes, probably influenced the amounts of RNA, DNA, and proteins released into the blood. On the other hand, the small cohort size for both groups might also be an explanation for these observations. Therefore, our findings have to be validated in a larger cohort.

Currently, patients need to receive a tumor-specific therapy at least 4 to 6 weeks, before conventional radiographic tumor assessments can reliably determine a tumor response. From a clinical perspective, identification of non-responders using a marker or marker panel that is able to indicate success or failure of a therapy at an early stage is highly warranted. The use of such marker panels might help to adjust treatment earlier than currently done using radiographic tumor assessments and, thereby, avoid or shorten side effects and adverse events of ineffective treatment. Consequently, early detection of therapy success would lead to a better quality of life especially for patients in late stages of tumor disease. Furthermore, an early adaption of therapy concept might impact the progression-free or

overall survival of patients. To our knowledge, except for the detection of mutations, no studies have used these very early time points for prediction of therapy response in NSCLC before.

## 4. Material and Methods

### 4.1. Study Design and Patient Biospecimen

The early response biomarker study was a part of the early response trial (ERT), a multicenter study funded by the German Center for Lung Research (DZL). This biomarker study was conducted in accordance with the Reporting Recommendations for Tumor Marker Prognostic Studies (REMARK) [47]. Serum and plasma samples were provided by Lung Biobank Heidelberg, Hannover Unified Biobank HUB, and UGMLC-Giessen Biobank, members of the Biobank platform of the German Center for Lung Research (DZL). The use of biomaterial and data for this study was approved by the local ethics committee of the Medical Faculty Heidelberg (S-445/2015). All patients included in the study signed informed consent and the study performed according to the principles set out in the WMA Declaration of Helsinki. We investigated blood from 50 stage IV patients with NSCLC (Table 1). Patients were selected by clinicians requiring MRI and measurable tumor size of at least 2 cm. All patients suffered from NSCLC and were selected by recommended therapy concept according to the current guidelines. Group A ( $n = 25$ ) received conventional chemotherapy since no targetable molecular alteration was detected during routine diagnostics. Group B ( $n = 25$ ) contained patients with a targetable driver mutation or gene fusion (see patients' characteristics, Table 1). First blood sample was collected within 24 h prior to therapy start (day  $-1$ , Figure 1). Due to different therapy concepts, blood samples were collected at different time points after therapy start. For chemotherapy group (group A), one post-treatment sample was collected at day  $+1$ , while two blood samples were assembled at day  $+7$  and  $+14$  for the TKI group (group B, Figure 1). Time points were selected due to literature search and own observations [35] that intravenous uptake of drugs can be faster compared to oral medication [48]. Routine computed tomography (CT) was performed at baseline and at time point of first clinical restaging (in median after 50 days). Tumor load change (primary and metastasized sites) was assessed by an experienced radiologist according to RECIST v 1.1 as size change of the tumor at time point of therapy start and at restaging.

### 4.2. DNA Extraction and Analysis by Digital PCR

cfDNA was extracted from one mL aliquots of frozen plasma with the QIAamp circulating nucleic acid kit (Qiagen, Hilden, Germany), following the manufacturer's recommendations for the purification of circulating nucleic acids. DNA quality was assessed with the Bioanalyzer 2100 using the High Sensitivity DNA Kit (Agilent Technologies, Santa Clara, CA, USA). DNA was quantified using the Qubit dsDNA HS Assay Kit with the Qubit 2.0 fluorometer (Thermo Fisher Scientific, Waltham, MA, USA). cfDNA was subjected to the measurement of known sensitizing EGFR mutations by digital PCR (dPCR) and TaqMan liquid biopsy dPCR assays EGFR\_6223, EGFR\_6224 and EGFR\_6225 (Thermo Fisher Scientific, Waltham, MA, USA), following the manufacturer's protocol. For echinoderm microtubule associated protein-like 4 (EML4)-ALK fusion and Serine/threonine-protein kinase B-raf (rapidly accelerated fibrosarcoma) (BRAF) mutation, no assay was available. Samples were measured as technical triplicates using the QuantStudio 3D digital PCR instrument and subsequently analyzed with the QuantStudio 3D AnalysisSuite Software (Thermo Fisher Scientific, Waltham, MA, USA). Reported mutated copies per  $\mu\text{L}$  reaction volume were extrapolated to mutant copies/mL plasma.

### 4.3. miRNA Extraction and Analysis by Quantitative Reverse-Transcription PCR

For this study, we selected 17 miRNAs that have been described in literature to be diagnostic and/or prognostic/predictive indicators when measured from plasma/serum of patients (Table A1). Circulating miRNAs were extracted from one milliliter aliquots of frozen plasma. Each plasma sample was spiked with  $4.8\text{E}+08$  copies of *cel-miR-54* to assess isolation efficiency. The isolation

was performed using the QIAamp circulating nucleic acid kit (Qiagen, Hilden, Germany), following the manufacturer's recommendations for the purification of circulating miRNAs. Isolated miRNAs were reverse transcribed (RT) with the TaqMan microRNA reverse transcription kit and reverse-transcription primers of the TaqMan microRNA assay kits for miRNAs *hsa-miR-21-5p*, *hsa-miR-214-3p*, *hsa-miR-23a-3p*, *hsa-miR-221-3p*, *hsa-miR-222-3p*, *hsa-miR-134-5p*, *hsa-miR-126-3p*, *hsa-miR-103-3p*, *let-7e-5p*, *hsa-miR342-3p*, *hsa-miR-1290*, *hsa-miR-223-3p*, *hsa-miR-20a-5p*, *hsa-miR-145-5p*, *hsa-miR-628-3p*, *hsa-miR-29c-3p*, *hsa-miR-210-3p*, *hsa-miR191*, and *hsa-miR-451a* (Thermo Fisher Scientific, Waltham, MA, USA). The qPCR reaction was conducted as technical triplicates in 384-well plates with the RT product, Premix Ex Taq master mix (Takara Bio, Kusatsu, Japan) and TaqMan probes for each miRNA using the LightCycler480 instrument (Roche Diagnostics, Basel, Switzerland). Reverse transcription and qPCR were performed following the manufacturer's protocol. miRNA abundances were normalized to the abundance of *hsa-miR-191*, which has been shown to be highly detectable in plasma and recommended to be used as housekeeper miRNA [43,49], within each sample.

#### 4.4. Measurement of Cytokeratin 18 (M30 and M65 Determination)

M30 and M65 levels in Ethylenediaminetetraacetic acid (EDTA)-Plasma were determined with M30 Apoptosense and M65 ELISA kits (PEVIVA, Tecomedical, Buende, Germany) according to the manufacturer's protocol. The samples were undiluted or diluted by a factor 2. The assay range was 0–1000 U/L for M30 and 0–2000 U/L for M65. For M30, units were defined using a recombinant protein standard. For M65, the units were defined using a synthetic peptide containing M6 and M5 epitope. 1 U/L = 1.24 pM.

#### 4.5. Determination of GSH and oxGSH Concentrations

GSH and oxGSH were detected with the competitive EIA kits "All species Glutathione ELISA kit" and "Human Oxidized Glutathione ELISA kit" from LSBio (Seattle, Washington, USA) according to the manufacturer's protocol. EDTA-plasma samples were diluted by a factor of 2 with sample diluent. For analysis, the data were linearized by plotting them on logarithmic axes. The detection range was 1.23–100 µg/mL with a sensitivity of 0.45 µg/mL for GSH and 4.688–300 pg/mL with a sensitivity of 2.8 pg/mL for oxGSH.

#### 4.6. Measurement of Glycodelin

Glycodelin levels in sera were detected using an enzyme-linked immunosorbent assay kit (ELISA BS-30-20, Bioserv Diagnostics, Rostock, Germany) with 50 µL of each serum in two technical replicates. The readout and standard curve were performed with ELISA Reader (Tecan Group Ltd., Crailsheim, Germany). ELISA results were visualized with GraphPad Prism 5 (GraphPad Software, San Diego, CA, USA).

#### 4.7. Statistical Analyses

The patient cohort was described using median and range for continuous variables and using absolute and relative frequencies for categorical variables. Furthermore, tumor response for each patient (in % RECIST) was descriptively illustrated by a waterfall plot. Afterward, correlations between individual biomarkers and tumor load at baseline were assessed using Pearson correlation coefficient. Examining the predictive value of single markers at the three time points, a univariate linear regression model was build comprising the variable "relative tumor load change from baseline to first CT after therapy" as a dependent variable for each biomarker and time point. Furthermore, for each time point, correlations between the biomarker were assessed using Pearson correlation coefficient and were illustrated by heatmaps. To create marker panels for the prognosis of relative tumor load change, a five-step forward regression analysis (based on the Akaike Information Criterion, AIC) was performed to find the marker panel consisting of biomarkers with the best predictive performance for each point in time. Due to the exploratory character of the study, *p*-values have a descriptive meaning and are not

adjusted for multiplicity. *p*-values <0.05 are defined as statistically significant. Furthermore, no missing values were imputed. All analyses were performed using R version 3.5.1 (<https://www.r-project.org>) and Graph Pad Prism Version 5 (GraphPad Software, San Diego, CA, USA).

## 5. Conclusions

For the first time, we investigated a panel of liquid biomarkers at three very early time points after therapy initiation (day +1, day +7, and day +14) for their predictive value. We found three individual marker panels including five biomarkers each at every time point with correlation rates  $R^2 > 0.71$  to tumor load change. These marker panels highly implicate that the efficiency of a specific NSCLC therapy can already be measured at very early time points after therapy start and might help to avoid or shorten side effects and adverse events of ineffective treatment.

**Author Contributions:** Conceptualization, F.B., C.P.H., H.S., T.M., S.J., M.M., and M.A.S.; data curation, C.P.H., G.H., C.F.S., S.R., H.G., A.G., and S.J.; formal analysis, M.F.; funding acquisition, F.B., C.P.H., M.T., H.G., A.G., and M.M.; investigation, F.J., S.W., S.D., and M.A.S.; methodology, F.B., H.S., and M.A.S.; project administration, M.M. and M.A.S.; supervision, M.A.S.; visualization, F.J., M.F., and M.A.S.; writing—original draft, F.J., F.B., S.W., S.J., and M.A.S.; writing—review and editing, F.J., F.B., S.W., S.D., C.P.H., G.H., C.F.S., S.R., M.F., M.T., H.G., A.G., H.S., T.M., S.J., M.M., and M.A.S. All authors have read and agreed to the published version of the manuscript.

**Funding:** This study was supported in part by the German Centre for Lung Research (grant numbers 82DZL14A2 and 82DZLR24A2).

**Acknowledgments:** We are grateful to Andrea Bopp, Ingrid Heinzmann-Groth, Karin Schnorr-Teichert, and Saskia Oestinger for the processing of blood samples.

**Conflicts of Interest:** M.M. and S.J. report grants from the German Center for Lung Research during the conduct of the study. T.M. reports grants and personal fees from the German Center for Lung Research (DZL) during the conduct of the study and grants and personal fees from Roche outside the submitted work. M.A.S. reports grants and personal fees from the German Center for Lung Research (DZL) during the conduct of the study. C.P.H. reports personal fees from Novartis, personal fees from Basilea, personal fees from Bayer, outside the submitted work. M.T. reports grants and personal fees from Celgene, personal fees from AbbVie, grants, personal fees, and non-financial support from Bristol-Myers Squibb, personal fees and non-financial support from Boehringer, personal fees from Lilly, personal fees and non-financial support from MSD, personal fees and non-financial support from Novartis, grants and personal fees from Roche, grants from AstraZeneca outside the submitted work. F.B. reports research funding from BMS, AstraZeneca, and Roche, personal honoraria from Novartis, MSD, Roche, AstraZeneca outside the submitted work. H.S. reports receiving support in research funding and honoraria from Roche. The other authors declare no potential conflicts of interest.

## Abbreviation List

BRAF	Serine/threonine-protein kinase B-raf (rapidly accelerated fibrosarcoma)
cfDNA	Cell-free DNA
CK-18	Cytokeratin 18
CT	Computer tomography
ctDNA	Circulating tumor DNA
CTx	Platinum-based chemotherapy
ECOG	Eastern Cooperative Oncology Performance Status Scale
EGFR	Epidermal growth factor receptor
EML4-ALK	Echinoderm microtubule associated protein-like 4-anaplastic lymphoma kinase
GSH	Glutathione
M30	Caspase-cleaved cytokeratin 18
M65	Full-length cytokeratin 18
miRNA	MicroRNA
MRI	Magnetic resonance imaging
NOS	Non other specified
NSCLC	Non-small cell lung cancer
oxGSH	Oxidized glutathione

PD	Progressive disease
PDL1	Programmed death ligand 1
PR	Partial remission
RECIST-1.1	Response Evaluation Criteria in Solid Tumors, version 1.1
SD	Stable disease
TKI	Tyrosine-kinase-inhibitor

## Appendix A Appendix

**Table A1.** microRNA overview and selection criteria; miRNAs were selected based on previous studies describing their (i) application for serum/plasma-based differentiation of NSCLC patients from healthy individuals and (ii) association to platinum-based and EGFR-TKI therapy studied in NSCLC cell lines or serum/plasma samples.

miRNA	Serum/Plasma Abundance in NSCLC Compared to Healthy Individuals	Association to Therapy		Reference
		Therapy Type	Effect Observed	
<i>miR-21-5p</i>	High	Platinum-based chemotherapy	High abundance in plasma is predictive for therapy resistance	[50]
<i>miR-214-3p</i>	High	EGFR-TKI therapy	High abundance in plasma of EGFR-TKI-resistant patients	[51]
<i>miR-23a-3p</i>	High	-	-	[52]
<i>miR-103-3p</i>	High	EGFR-TKI therapy	High abundance in gefitinib-resistant cell lines	[53,54]
<i>miR-221-3p</i>				
<i>miR-222-3p</i>	-	EGFR-TKI therapy	High abundance in gefitinib-resistant cell lines	[55]
<i>miR-134-5p</i>				
<i>miR-126-3p</i>	Low	EGFR-TKI therapy	High abundance in gefitinib-sensitive cell lines	[56,57]
<i>let-7e-5p</i>	Low	-	-	[58]
<i>miR-342-3p</i>	Low	EGFR-TKI therapy	High abundance in gefitinib-resistant cell lines	[59]
<i>miR-1290</i>	High	EGFR-TKI therapy	Longitudinal monitoring of EGFR-TKI therapy from serum	[33]
<i>miR-223-3p</i>	High	EGFR-TKI therapy	High abundance in erlotinib-sensitive cell lines	[60,61]
<i>miR-20a-5p</i>	High	EGFR-TKI therapy	Increased plasma abundance in EGFRmut compared to EGFR wild-type patients	[60,62]
<i>miR-145-5p</i>	High	EGFR-TKI therapy	High abundance in gefitinib-sensitive cell lines	[57,60]
<i>miR-628-3p</i>	High	-	-	[63]
<i>miR-29c-3p</i>	High	Platinum-based chemotherapy	High abundance enhances chemotherapy sensitivity in cell lines	[64,65]
<i>miR-210-3p</i>	High	Platinum-based chemotherapy	Decreased serum abundance in patients responding to chemotherapy	[66]

**Table A2.** Quality control of blood samples; overview about risk of hemolysis in the plasma samples used for this study. Hemolysis was assessed using differences between *hsa-miR-451a* and *hsa-miR-23a-3p* with a Ct difference >7 being used as a cut-off for hemolytic samples. Lower values indicate little (5–7) or no (<5) risk of hemolysis [43]. For Patient\_37, material was not sufficient for miRNA and mutation analysis. Hence, risk of hemolysis could not be assessed in this sample.

	Patient_ID	Baseline	1st Follow-up	2nd Follow-up
Group A	Patient_01			-
	Patient_02			-
	Patient_03			-
	Patient_04			-
	Patient_05			-
	Patient_06			-
	Patient_07			-
	Patient_08			-
	Patient_09			-
	Patient_10			-
	Patient_11			-
	Patient_12			-
	Patient_13			-
	Patient_14			-
	Patient_15			-
	Patient_16			-
	Patient_17			-
	Patient_18			-
	Patient_19			-
	Patient_20			-
	Patient_21			-
	Patient_22			-
	Patient_23			-
	Patient_24			-
	Patient_25			-
Group B	Patient_26			
	Patient_27			
	Patient_28			
	Patient_29			
	Patient_30			
	Patient_31			
	Patient_32			
	Patient_33			
	Patient_34			
	Patient_35			
	Patient_36			
	Patient_37	NA	NA	NA
	Patient_38			
	Patient_39			
	Patient_40			
	Patient_41			
	Patient_42			
	Patient_43			
	Patient_44			
	Patient_45			
	Patient_46			
	Patient_47			
	Patient_48			
	Patient_49			
	Patient_50			
	<5	No risk of hemolysis		
	5 to 7	Sample is possibly affected by hemolysis		
	>7	High risk of hemolysis		
	NA	Not enough material available		

**Table A3.** Applicability of marker panels at individual time points.

Marker Panel	Day +1 (Group A)	Day +7 (Group B)	Day +14 (Group B)
	R2	R2	R2
Day +1	<b>0.78</b>	0.11	0.17
Day +7	0.06	<b>0.71</b>	0.25
Day +14	0.22	0.21	<b>0.71</b>

The five-marker panels from Figure 5A used at other assessed time points. R<sup>2</sup> values were calculated using a stepwise regression model.

## References

1. Siegel, R.L.; Miller, K.D.; Jemal, A. Cancer statistics, 2020. *CA Cancer J. Clin.* **2020**, *70*, 7–30. [[CrossRef](#)]
2. Shaw, A.T.; Yeap, B.Y.; Mino-Kenudson, M.; Digumarthy, S.R.; Costa, D.B.; Heist, R.S.; Solomon, B.; Stubbs, H.; Admane, S.; McDermott, U.; et al. Clinical features and outcome of patients with non-small-cell lung cancer who harbor EML4-ALK. *J. Clin. Oncol.* **2009**, *27*, 4247–4253. [[CrossRef](#)]
3. Girard, N. Optimizing outcomes in EGFR mutation-positive NSCLC: Which tyrosine kinase inhibitor and when? *Future Oncol.* **2018**, *14*, 1117–1132. [[CrossRef](#)]
4. Shaw, A.T.; Kim, D.W.; Nakagawa, K.; Seto, T.; Crino, L.; Ahn, M.J.; De Pas, T.; Besse, B.; Solomon, B.J.; Blackhall, F.; et al. Crizotinib versus chemotherapy in advanced ALK-positive lung cancer. *N. Engl. J. Med.* **2013**, *368*, 2385–2394. [[CrossRef](#)]
5. Yang, J.C.; Wu, Y.L.; Schuler, M.; Sebastian, M.; Popat, S.; Yamamoto, N.; Zhou, C.; Hu, C.P.; O’Byrne, K.; Feng, J.; et al. Afatinib versus cisplatin-based chemotherapy for EGFR mutation-positive lung adenocarcinoma (LUX-Lung 3 and LUX-Lung 6): Analysis of overall survival data from two randomised, phase 3 trials. *Lancet Oncol.* **2015**, *16*, 141–151. [[CrossRef](#)]
6. Mitsudomi, T.; Morita, S.; Yatabe, Y.; Negoro, S.; Okamoto, I.; Tsurutani, J.; Seto, T.; Satouchi, M.; Tada, H.; Hirashima, T.; et al. Gefitinib versus cisplatin plus docetaxel in patients with non-small-cell lung cancer harbouring mutations of the epidermal growth factor receptor (WJTOG3405): An open label, randomised phase 3 trial. *Lancet Oncol.* **2010**, *11*, 121–128. [[CrossRef](#)]
7. Westover, D.; Zugazagoitia, J.; Cho, B.C.; Lovly, C.M.; Paz-Ares, L. Mechanisms of acquired resistance to first- and second-generation EGFR tyrosine kinase inhibitors. *Ann. Oncol.* **2018**, *29*, i10–i19. [[CrossRef](#)] [[PubMed](#)]
8. Lin, J.J.; Riely, G.J.; Shaw, A.T. Targeting ALK: Precision medicine takes on drug resistance. *Cancer Discov.* **2017**, *7*, 137–155. [[CrossRef](#)] [[PubMed](#)]
9. Hickman, J.A.; Beere, H.M.; Wood, A.C.; Waters, C.M.; Parmar, R. Mechanisms of cytotoxicity caused by antitumour drugs. *Toxicol. Lett.* **1992**, *64–65*, 553–561. [[CrossRef](#)]
10. Meyn, R.E.; Stephens, L.C.; Hunter, N.R.; Milas, L. Apoptosis in murine tumors treated with chemotherapy agents. *Anticancer Drugs* **1995**, *6*, 443–450. [[CrossRef](#)] [[PubMed](#)]
11. Ellis, P.A.; Smith, I.E.; McCarthy, K.; Detre, S.; Salter, J.; Dowsett, M. Preoperative chemotherapy induces apoptosis in early breast cancer. *Lancet* **1997**, *349*, 849. [[CrossRef](#)]
12. Lee, J.Y.; Qing, X.; Xiumin, W.; Yali, B.; Chi, S.; Bak, S.H.; Lee, H.Y.; Sun, J.M.; Lee, S.H.; Ahn, J.S.; et al. Longitudinal monitoring of EGFR mutations in plasma predicts outcomes of NSCLC patients treated with EGFR TKIs: Korean lung cancer consortium (KLCC-12-02). *Oncotarget* **2016**, *7*, 6984–6993. [[CrossRef](#)] [[PubMed](#)]
13. Sorensen, B.S.; Wu, L.; Wei, W.; Tsai, J.; Weber, B.; Nexø, E.; Meldgaard, P. Monitoring of epidermal growth factor receptor tyrosine kinase inhibitor-sensitizing and resistance mutations in the plasma DNA of patients with advanced non-small cell lung cancer during treatment with erlotinib. *Cancer* **2014**, *120*, 3896–3901. [[CrossRef](#)] [[PubMed](#)]
14. Iorio, M.V.; Croce, C.M. MicroRNA dysregulation in cancer: Diagnostics, monitoring and therapeutics. A comprehensive review. *EMBO Mol. Med.* **2017**, *9*, 852. [[CrossRef](#)]
15. Jung, M.; Schaefer, A.; Steiner, I.; Kempkensteffen, C.; Stephan, C.; Erbersdobler, A.; Jung, K. Robust microRNA stability in degraded RNA preparations from human tissue and cell samples. *Clin. Chem.* **2010**, *56*, 998–1006. [[CrossRef](#)]

16. Mitchell, P.S.; Parkin, R.K.; Kroh, E.M.; Fritz, B.R.; Wyman, S.K.; Pogosova-Agadjanyan, E.L.; Peterson, A.; Noteboom, J.; O'Briant, K.C.; Allen, A.; et al. Circulating microRNAs as stable blood-based markers for cancer detection. *Proc. Natl. Acad. Sci. USA* **2008**, *105*, 10513–10518. [[CrossRef](#)]
17. Leers, M.P.; Kolgen, W.; Bjorklund, V.; Bergman, T.; Tribbick, G.; Persson, B.; Bjorklund, P.; Ramaekers, F.C.; Bjorklund, B.; Nap, M.; et al. Immunocytochemical detection and mapping of a cytokeratin 18 neo-epitope exposed during early apoptosis. *J. Pathol.* **1999**, *187*, 567–572. [[CrossRef](#)]
18. Crosbie, P.A.; Shah, R.; Summers, Y.; Dive, C.; Blackhall, F. Prognostic and predictive biomarkers in early stage NSCLC: CTCs and serum/plasma markers. *Transl. Lung Cancer Res.* **2013**, *2*, 382–397.
19. Couto, N.; Wood, J.; Barber, J. The role of glutathione reductase and related enzymes on cellular redox homeostasis network. *Free Radic. Biol. Med.* **2016**, *95*, 27–42. [[CrossRef](#)]
20. Plowright, L.; Harrington, K.J.; Pandha, H.S.; Morgan, R. HOX transcription factors are potential therapeutic targets in non-small-cell lung cancer (targeting HOX genes in lung cancer). *Br. J. Cancer* **2009**, *100*, 470–475. [[CrossRef](#)]
21. Lee, C.L.; Lam, K.K.; Koistinen, H.; Seppala, M.; Kurpisz, M.; Fernandez, N.; Pang, R.T.; Yeung, W.S.; Chiu, P.C. Glycodelin-A as a paracrine regulator in early pregnancy. *J. Reprod. Immunol.* **2011**, *90*, 29–34. [[CrossRef](#)] [[PubMed](#)]
22. Alok, A.; Karande, A.A. The role of glycodelin as an immune-modulating agent at the feto-maternal interface. *J. Reprod. Immunol.* **2009**, *83*, 124–127. [[CrossRef](#)] [[PubMed](#)]
23. Bischof, A.; Briese, V.; Richter, D.U.; Bergemann, C.; Friese, K.; Jeschke, U. Measurement of glycodelin A in fluids of benign ovarian cysts, borderline tumours and malignant ovarian cancer. *Anticancer Res.* **2005**, *25*, 1639–1644. [[PubMed](#)]
24. Kamarainen, M.; Halttunen, M.; Koistinen, R.; von Boguslawsky, K.; von Smitten, K.; Andersson, L.C.; Seppala, M. Expression of glycodelin in human breast and breast cancer. *Int. J. Cancer* **1999**, *83*, 738–742. [[CrossRef](#)]
25. Ren, S.; Liu, S.; Howell, P.M., Jr.; Zhang, G.; Pannell, L.; Samant, R.; Shevde-Samant, L.; Tucker, J.A.; Fodstad, O.; Riker, A.I. Functional characterization of the progestagen-associated endometrial protein gene in human melanoma. *J. Cell. Mol. Med.* **2010**, *14*, 1432–1442. [[CrossRef](#)]
26. Schneider, M.A.; Granzow, M.; Warth, A.; Schnabel, P.A.; Thomas, M.; Herth, F.J.; Dienemann, H.; Muley, T.; Meister, M. Glycodelin: A new biomarker with immunomodulatory functions in non-small cell lung cancer. *Clin. Cancer Res. Off. J. Am. Assoc. Cancer Res.* **2015**, *21*, 3529–3540. [[CrossRef](#)]
27. Schneider, M.A.; Muley, T.; Weber, R.; Wessels, S.; Thomas, M.; Herth, F.J.F.; Kahn, N.C.; Eberhardt, R.; Winter, H.; Heussel, G.; et al. Glycodelin as a serum and tissue biomarker for metastatic and advanced NSCLC. *Cancers* **2018**, *10*, 486. [[CrossRef](#)]
28. Gamcsik, M.P.; Kasibhatla, M.S.; Teeter, S.D.; Colvin, O.M. Glutathione levels in human tumors. *Biomarkers* **2012**, *17*, 671–691. [[CrossRef](#)]
29. Kramer, G.; Erdal, H.; Mertens, H.J.; Nap, M.; Mauermann, J.; Steiner, G.; Marberger, M.; Biven, K.; Shoshan, M.C.; Linder, S. Differentiation between cell death modes using measurements of different soluble forms of extracellular cytokeratin 18. *Cancer Res.* **2004**, *64*, 1751–1756. [[CrossRef](#)]
30. Yang, P.; Ebbert, J.O.; Sun, Z.; Weinshilboum, R.M. Role of the glutathione metabolic pathway in lung cancer treatment and prognosis: A review. *J. Clin. Oncol.* **2006**, *24*, 1761–1769. [[CrossRef](#)]
31. Tang, C.H.; Parham, C.; Shocron, E.; McMahon, G.; Patel, N. Picoplatin overcomes resistance to cell toxicity in small-cell lung cancer cells previously treated with cisplatin and carboplatin. *Cancer Chemother. Pharmacol.* **2011**, *67*, 1389–1400. [[CrossRef](#)] [[PubMed](#)]
32. Zhang, H.; Mao, F.; Shen, T.; Luo, Q.; Ding, Z.; Qian, L.; Huang, J. Plasma miR-145, miR-20a, miR-21 and miR-223 as novel biomarkers for screening early-stage non-small cell lung cancer. *Oncol. Lett.* **2017**, *13*, 669–676. [[CrossRef](#)] [[PubMed](#)]
33. Zhang, W.C.; Chin, T.M.; Yang, H.; Nga, M.E.; Lunny, D.P.; Lim, E.K.; Sun, L.L.; Pang, Y.H.; Leow, Y.N.; Malusay, S.R.; et al. Tumour-initiating cell-specific miR-1246 and miR-1290 expression converge to promote non-small cell lung cancer progression. *Nat. Commun.* **2016**, *7*, 11702. [[CrossRef](#)]
34. Abbosh, C.; Birkbak, N.J.; Wilson, G.A.; Jamal-Hanjani, M.; Constantin, T.; Salari, R.; Le Quesne, J.; Moore, D.A.; Veeriah, S.; Rosenthal, R.; et al. Phylogenetic ctDNA analysis depicts early-stage lung cancer evolution. *Nature* **2017**, *545*, 446–451. [[CrossRef](#)] [[PubMed](#)]



35. Riediger, A.L.; Dietz, S.; Schirmer, U.; Meister, M.; Heinzmann-Groth, I.; Schneider, M.; Muley, T.; Thomas, M.; Sultmann, H. Mutation analysis of circulating plasma DNA to determine response to EGFR tyrosine kinase inhibitor therapy of lung adenocarcinoma patients. *Sci. Rep.* **2016**, *6*, 33505. [[CrossRef](#)] [[PubMed](#)]
36. Rijavec, E.; Coco, S.; Genova, C.; Rossi, G.; Longo, L.; Grossi, F. Liquid biopsy in non-small cell lung cancer: Highlights and challenges. *Cancers* **2019**, *12*, 17. [[CrossRef](#)]
37. Scott, A.; Salgia, R. Biomarkers in lung cancer: From early detection to novel therapeutics and decision making. *Biomark. Med.* **2008**, *2*, 577–586. [[CrossRef](#)]
38. Hassanein, M.; Callison, J.C.; Callaway-Lane, C.; Aldrich, M.C.; Grogan, E.L.; Massion, P.P. The state of molecular biomarkers for the early detection of lung cancer. *Cancer Prev. Res. (Phila)* **2012**, *5*, 992–1006. [[CrossRef](#)]
39. Calabrese, F.; Lunardi, F.; Pezzuto, F.; Fortarezza, F.; Vuljan, S.E.; Marquette, C.; Hofman, P. Are there new biomarkers in tissue and liquid biopsies for the early detection of non-small cell lung cancer? *J. Clin. Med.* **2019**, *8*, 414. [[CrossRef](#)]
40. Goldberg, S.B.; Narayan, A.; Kole, A.J.; Decker, R.H.; Teysir, J.; Carriero, N.J.; Lee, A.; Nemati, R.; Nath, S.K.; Mane, S.M.; et al. Early assessment of lung cancer immunotherapy response via circulating tumor DNA. *Clin. Cancer Res. Off. J. Am. Assoc. Cancer Res.* **2018**, *24*, 1872–1880. [[CrossRef](#)]
41. Wei, J.; Gao, W.; Zhu, C.J.; Liu, Y.Q.; Mei, Z.; Cheng, T.; Shu, Y.Q. Identification of plasma microRNA-21 as a biomarker for early detection and chemosensitivity of non-small cell lung cancer. *Chin. J. Cancer* **2011**, *30*, 407–414. [[CrossRef](#)] [[PubMed](#)]
42. Marchetti, A.; Palma, J.F.; Felicioni, L.; De Pas, T.M.; Chiari, R.; Del Grammastro, M.; Filice, G.; Ludovini, V.; Brandes, A.A.; Chella, A.; et al. Early prediction of response to tyrosine kinase inhibitors by quantification of EGFR mutations in plasma of NSCLC patients. *J. Thorac. Oncol.* **2015**, *10*, 1437–1443. [[CrossRef](#)] [[PubMed](#)]
43. Blondal, T.; Jensby Nielsen, S.; Baker, A.; Andreassen, D.; Mouritzen, P.; Wrang Teilum, M.; Dahlsveen, I.K. Assessing sample and miRNA profile quality in serum and plasma or other biofluids. *Methods* **2013**, *59*, S1–S6. [[CrossRef](#)] [[PubMed](#)]
44. Oxnard, G.R.; Paweletz, C.P.; Kuang, Y.; Mach, S.L.; O’Connell, A.; Messineo, M.M.; Luke, J.J.; Butaney, M.; Kirschmeier, P.; Jackman, D.M.; et al. Noninvasive detection of response and resistance in EGFR-mutant lung cancer using quantitative next-generation genotyping of cell-free plasma DNA. *Clin. Cancer Res. Off. J. Am. Assoc. Cancer Res.* **2014**, *20*, 1698–1705. [[CrossRef](#)] [[PubMed](#)]
45. Douillard, J.Y.; Ostoros, G.; Cobo, M.; Ciuleanu, T.; Cole, R.; McWalter, G.; Walker, J.; Dearden, S.; Webster, A.; Milenkova, T.; et al. Gefitinib treatment in EGFR mutated caucasian NSCLC: Circulating-free tumor DNA as a surrogate for determination of EGFR status. *J. Thorac. Oncol.* **2014**, *9*, 1345–1353. [[CrossRef](#)]
46. De Petris, L.; Branden, E.; Herrmann, R.; Sanchez, B.C.; Koyi, H.; Linderholm, B.; Lewensohn, R.; Linder, S.; Lehtio, J. Diagnostic and prognostic role of plasma levels of two forms of cytokeratin 18 in patients with non-small-cell lung cancer. *Eur. J. Cancer* **2011**, *47*, 131–137. [[CrossRef](#)]
47. McShane, L.M.; Altman, D.G.; Sauerbrei, W.; Taube, S.E.; Gion, M.; Clark, G.M. Reporting recommendations for tumor marker prognostic studies. *J. Clin. Oncol.* **2005**, *23*, 9067–9072. [[CrossRef](#)]
48. Joel, S.P.; Clark, P.I.; Heap, L.; Webster, L.; Robbins, S.; Craft, H.; Slevin, M.L. Pharmacological attempts to improve the bioavailability of oral etoposide. *Cancer Chemother. Pharmacol.* **1995**, *37*, 125–133. [[CrossRef](#)]
49. Peltier, H.J.; Latham, G.J. Normalization of microRNA expression levels in quantitative RT-PCR assays: Identification of suitable reference RNA targets in normal and cancerous human solid tissues. *RNA* **2008**, *14*, 844–852. [[CrossRef](#)]
50. Zhu, J.; Qi, Y.; Wu, J.; Shi, M.; Feng, J.; Chen, L. Evaluation of plasma microRNA levels to predict insensitivity of patients with advanced lung adenocarcinomas to pemetrexed and platinum. *Oncol. Lett.* **2016**, *12*, 4829–4837. [[CrossRef](#)]
51. Liao, J.; Lin, J.; Lin, D.; Zou, C.; Kurata, J.; Lin, R.; He, Z.; Su, Y. Down-regulation of miR-214 reverses erlotinib resistance in non-small-cell lung cancer through up-regulating LHX6 expression. *Sci. Rep.* **2017**, *7*, 781. [[CrossRef](#)] [[PubMed](#)]
52. Hetta, H.F.; Zahran, A.M.; Shafik, E.A.; El-Mahdy, R.I.; Mohamed, N.A.; Nabil, E.E.; Esmael, H.M.; Alkady, O.A.; Elkady, A.; Mohareb, D.A.; et al. Circulating miRNA-21 and miRNA-23a expression signature as potential biomarkers for early detection of non-small-cell lung cancer. *Microrna* **2019**, *8*, 206–215. [[CrossRef](#)] [[PubMed](#)]

53. Lv, S.; Xue, J.; Wu, C.; Wang, L.; Wu, J.; Xu, S.; Liang, X.; Lou, J. Identification of a panel of serum microRNAs as biomarkers for early detection of lung adenocarcinoma. *J. Cancer* **2017**, *8*, 48–56. [[CrossRef](#)]
54. Garofalo, M.; Romano, G.; Di Leva, G.; Nuovo, G.; Jeon, Y.J.; Ngankeu, A.; Sun, J.; Lovat, F.; Alder, H.; Condorelli, G.; et al. EGFR and MET receptor tyrosine kinase-altered microRNA expression induces tumorigenesis and gefitinib resistance in lung cancers. *Nat. Med.* **2011**, *18*, 74–82. [[CrossRef](#)] [[PubMed](#)]
55. Kitamura, K.; Seike, M.; Okano, T.; Matsuda, K.; Miyana, A.; Mizutani, H.; Noro, R.; Minegishi, Y.; Kubota, K.; Gemma, A. MiR-134/487b/655 cluster regulates TGF-beta-induced epithelial-mesenchymal transition and drug resistance to gefitinib by targeting MAGI2 in lung adenocarcinoma cells. *Mol. Cancer Ther.* **2014**, *13*, 444–453. [[CrossRef](#)] [[PubMed](#)]
56. Sanfiorenzo, C.; Ilie, M.I.; Belaid, A.; Barlesi, F.; Mouroux, J.; Marquette, C.H.; Brest, P.; Hofman, P. Two panels of plasma microRNAs as non-invasive biomarkers for prediction of recurrence in resectable NSCLC. *PLoS ONE* **2013**, *8*, e54596. [[CrossRef](#)] [[PubMed](#)]
57. Zhong, M.; Ma, X.; Sun, C.; Chen, L. MicroRNAs reduce tumor growth and contribute to enhance cytotoxicity induced by gefitinib in non-small cell lung cancer. *Chem. Biol. Interact.* **2010**, *184*, 431–438. [[CrossRef](#)]
58. Kumar, S.; Sharawat, S.K.; Ali, A.; Gaur, V.; Malik, P.S.; Kumar, S.; Mohan, A.; Guleria, R. Identification of differentially expressed circulating serum microRNA for the diagnosis and prognosis of Indian non-small cell lung cancer patients. *Curr. Probl. Cancer* **2020**, 100540. [[CrossRef](#)]
59. Zheng, F.; Zhang, H.; Lu, J. Identification of potential microRNAs and their targets in promoting gefitinib resistance by integrative network analysis. *J. Thorac. Dis.* **2019**, *11*, 5535–5546. [[CrossRef](#)]
60. Geng, Q.; Fan, T.; Zhang, B.; Wang, W.; Xu, Y.; Hu, H. Five microRNAs in plasma as novel biomarkers for screening of early-stage non-small cell lung cancer. *Respir. Res.* **2014**, *15*, 149. [[CrossRef](#)]
61. Han, J.; Zhao, F.; Zhang, J.; Zhu, H.; Ma, H.; Li, X.; Peng, L.; Sun, J.; Chen, Z. miR-223 reverses the resistance of EGFR-TKIs through IGF1R/PI3K/Akt signaling pathway. *Int. J. Oncol.* **2016**, *48*, 1855–1867. [[CrossRef](#)] [[PubMed](#)]
62. Qu, L.; Li, L.; Zheng, X.; Fu, H.; Tang, C.; Qin, H.; Li, X.; Wang, H.; Li, J.; Wang, W.; et al. Circulating plasma microRNAs as potential markers to identify EGFR mutation status and to monitor epidermal growth factor receptor-tyrosine kinase inhibitor treatment in patients with advanced non-small cell lung cancer. *Oncotarget* **2017**, *8*, 45807–45824. [[CrossRef](#)]
63. Wang, Y.; Zhao, H.; Gao, X.; Wei, F.; Zhang, X.; Su, Y.; Wang, C.; Li, H.; Ren, X. Identification of a three-miRNA signature as a blood-borne diagnostic marker for early diagnosis of lung adenocarcinoma. *Oncotarget* **2016**, *7*, 26070–26086. [[CrossRef](#)] [[PubMed](#)]
64. Yang, X.; Zhang, Q.; Zhang, M.; Su, W.; Wang, Z.; Li, Y.; Zhang, J.; Beer, D.G.; Yang, S.; Chen, G. Serum microRNA signature is capable of early diagnosis for non-small cell lung cancer. *Int. J. Biol. Sci.* **2019**, *15*, 1712–1722. [[CrossRef](#)] [[PubMed](#)]
65. Sun, D.M.; Tang, B.F.; Li, Z.X.; Guo, H.B.; Cheng, J.L.; Song, P.P.; Zhao, X. MiR-29c reduces the cisplatin resistance of non-small cell lung cancer cells by negatively regulating the PI3K/Akt pathway. *Sci. Rep.* **2018**, *8*, 8007. [[CrossRef](#)] [[PubMed](#)]
66. Li, Z.H.; Zhang, H.; Yang, Z.G.; Wen, G.Q.; Cui, Y.B.; Shao, G.G. Prognostic significance of serum microRNA-210 levels in nonsmall-cell lung cancer. *J. Int. Med. Res.* **2013**, *41*, 1437–1444. [[CrossRef](#)]

